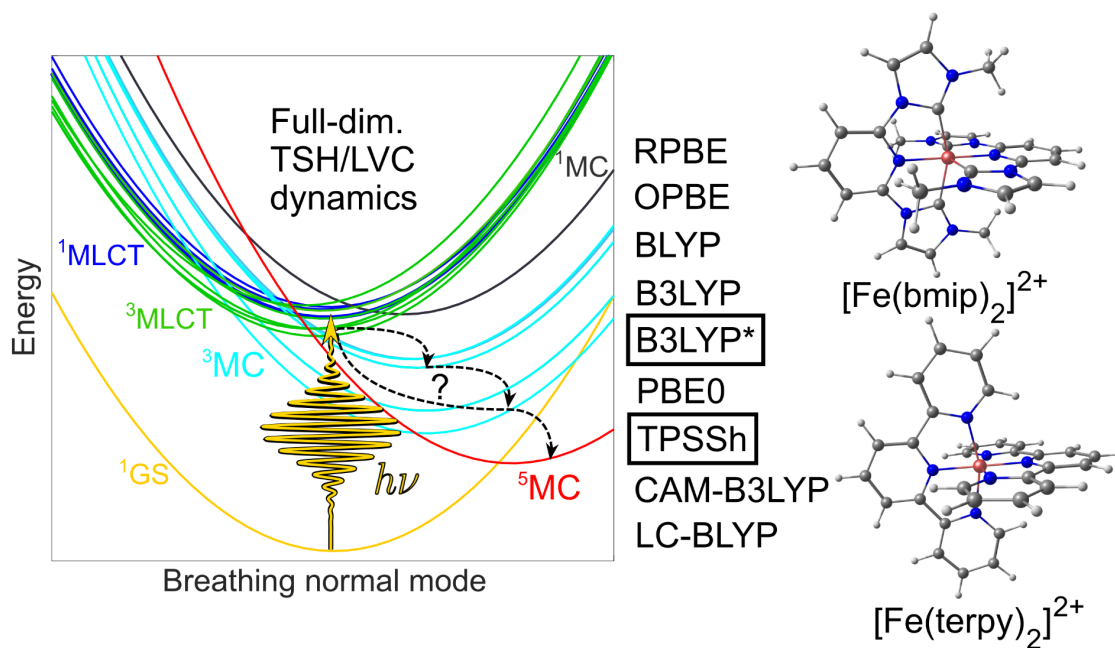


2024

## Assessing density functional excited-state descriptions by full-dimensional TSH dynamics simulations [1]

Ultrafast excited-state dynamics are at the heart of photofunctional molecules, determining their applicability and efficiency. Time-resolved (pump-probe) experiments utilizing ultrashort (ps-fs) pulses are powerful tools to resolve excited-state mechanisms, however, analysis of the obtained data can be problematic, often leading to contradictory interpretations. Theory — in particular time-dependent approaches — can deliver valuable excited-state data that might be difficult to access by experimental techniques, due to, e.g., limited time resolution and/or overlapping signals. The interplay of experiments and theory thus has a crucial importance in deciphering all details of the ultrafast dynamics.

One of the most important factors governing the accuracy of excited-dynamics simulations is the level of quantum chemistry. For the transition metal complexes studied by the group, the state of the art of electronic structure theory is still heavily dominated by (time-dependent) density functional theory (DFT/TD-DFT) methods. While being computationally rather efficient, the PESs obtained by these methods may highly depend on the chosen exchange-correlation functional, in particular, when electronic states with different spin multiplicities are considered. Herein, using full-dimensional trajectory surface hopping (TSH) dynamics simulations carried out on linear vibronic coupling (LVC) potentials, we assess the performance of various DFT/TD-DFT descriptions (RPBE, OPBE, BLYP, B3LYP, B3LYP\*, PBE0, TPSSh, CAM-B3LYP, and LC-BLYP). We exploit the existence of time-resolved X-ray emission spectroscopy (XES) data for the  $[\text{Fe}(\text{bmip})_2]^{2+}$  and  $[\text{Fe}(\text{terpy})_2]^{2+}$  prototypes for dynamics between metal-to-ligand charge transfer (MLCT) and metal-centered (MC) states (see Figure 1), which serve as a reference to benchmark the calculations (bmip = 2,6-bis(3-methylimidazole-1-ylidene)-pyridine, terpy = 2,2':6',2''-terpyridine). We base our assessment on identifying qualitative features and timescales in the simulated and experimentally extracted population dynamics. We consider our approach as an interesting alternative to contrasting full-dimensional DFT/TD-DFT dynamics against those carried out at higher level of quantum chemistry, such as CASPT2, which are currently not feasible for complexes such as  $[\text{Fe}(\text{bmip})_2]^{2+}$  and  $[\text{Fe}(\text{terpy})_2]^{2+}$ . The results show that the simulated ultrafast population dynamics between MLCT and MC states with various spin multiplicities (singlet, triplet, quintet, see Figure 1) highly depend on the utilized DFT/TD-DFT method with the percentage of exact (Hartree-Fock) exchange being the governing factor. Importantly, B3LYP\* and TPSSh are the only DFT/TD-DFT methods with a satisfactory performance, best reproducing the experimentally resolved dynamics for both complexes, signalling an optimal balance in the description of MLCT-MC energetics. This work demonstrates the power of combining TSH/LVC dynamics simulations with time-resolved experimental reference data to benchmark full-dimensional potential energy surfaces.



**Figure 1.** Graphical summary of the presented work: one-dimensional potential energy surfaces of Fe(II) complexes (left), the set of tested exchange-correlation functionals (middle), and molecular structure of

**References:**

- [1] M. Pápai, *Simulation of Ultrafast Excited-State Dynamics of Fe(II) Complexes: Assessment of Electronic Structure Descriptions*, *Journal of Chemical Theory and Computation*, DOI: 10.1021/acs.jctc.4c01331 (2025) <https://doi.org/10.1021/acs.jctc.4c01331>

**Developments** — The group has been continuously developing theoretical and experimental tools in order to investigate the ultrafast photoinduced dynamics in functional molecules, and to design new ones with improved performance. The experimental tools include pioneering static high-energy-resolution laboratory X-ray spectroscopy, with hard X-ray absorption being performed routinely and efficiently, while X-ray emission spectroscopy is still being optimized. Ultrafast studies with X-ray spectroscopy and scattering probes are carried out at synchrotron radiation sources and X-ray free electron lasers. In addition, we have realized in our home laboratory a femtosecond-resolved transient optical absorption spectroscopy station, and a femtosecond stimulated Raman scattering setup is being built. Our theoretical efforts focus on designing new functional molecules with quantum chemistry (which we later attempt to synthesize and then subject to experimental tests), as well as running (quantum) dynamics simulations to model the dynamics in light activated molecular systems. In what follows we report such works that were published in the previous year.

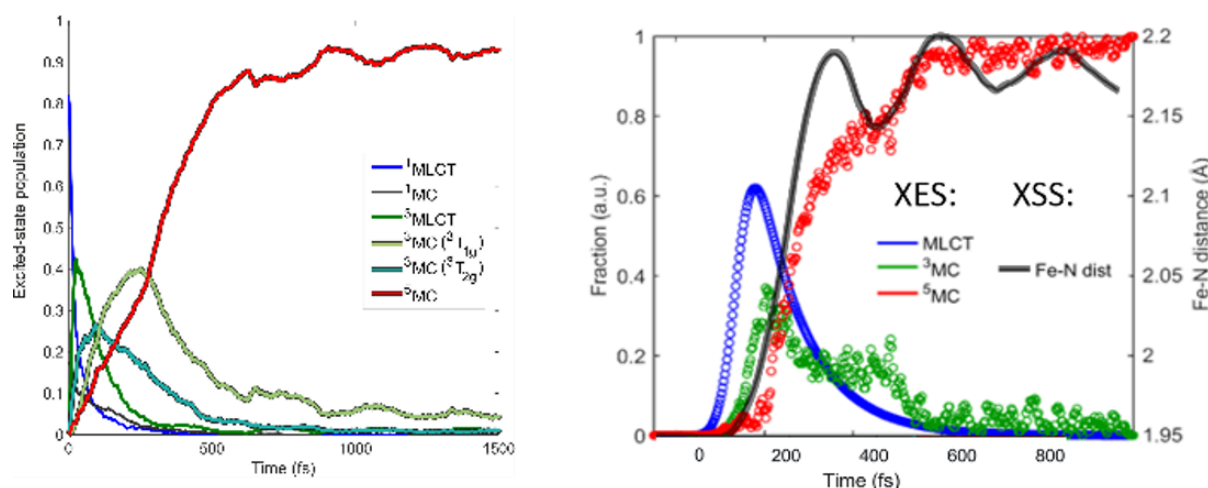


Figure 1. Comparison of the simulated excited-state dynamics of  $[\text{Fe}(\text{terpy})_2]^{2+}$  (left) vs the experimentally-extracted population (and vibrational) dynamics of  $[\text{Fe}(\text{bipy})_3]^{2+}$ . (Adapted from ref. 1)

**Excited-state dynamics in Fe(II) polypyridyl systems.** — We offered a solution to the long-debated mechanism of low-spin (LS, singlet)  $\rightarrow$  high-spin (HS, quintet) photoswitching in Fe(II) polypyridine complexes. Importantly, we simulated the entire singlet-triplet-quintet excited-state dynamics in full dimension for a prototypical Fe(II) polypyridine, namely, the base molecule of our group,  $[\text{Fe}(\text{terpy})_2]^{2+}$ . We report a branching mechanism involving the two triplet metal-centered ( $^3\text{MC}$ ) components,  $^3T_{1g}$  and  $^3T_{2g}$ . While the direct  $^3\text{MLCT} \rightarrow ^5\text{MC}$  (MLCT = metal-to-ligand charge transfer) mechanism is considered as a relevant alternative, we show that it could only be operative, and thus lead to competing pathways, in the absence of  $^3\text{MC}$  states. The quintet state is populated on the sub-picosecond timescale involving non-exponential dynamics and coherent Fe-N breathing oscillations. The results are in agreement with the available time-resolved experimental data on Fe(II) polypyridines (see Figure 1, in which we compare our results to those obtained by time-resolved experiments for  $[\text{Fe}(\text{bipy})_3]^{2+}$ ), and fully describe the photorelaxation dynamics.[1]

**Bicolor high-energy-resolution von Hámos XES spectrometer with conical analyzer.** — Besides the X-ray emission spectra of selected single elements offered by traditional high-energy-resolution spectrometers based on spherically or cylindrically bent analyzer single crystals, some experiments (like analyzing X-ray emission from plasma generated by ultrashort laser pulses) require the detection of XES of two elements simultaneously. To serve such cases, we have developed and benchmarked a von Hámos spectrometer based on a non-conventional conical Si single crystal analyzer. The analyzer was tested with different primary and secondary X-ray sources as well as a hard X-ray sensitive CCD camera. The spectrometer setup was also characterized with ray-tracing simulations. Both experimental and simulated results affirm that the conical spectrometer can efficiently detect and resolve the two pairs of two elements (Ni and Cu) K X-ray emission spectroscopy (XES) peaks simultaneously, requiring a less than 2 cm-wide array on a single position-sensitive detector [2].

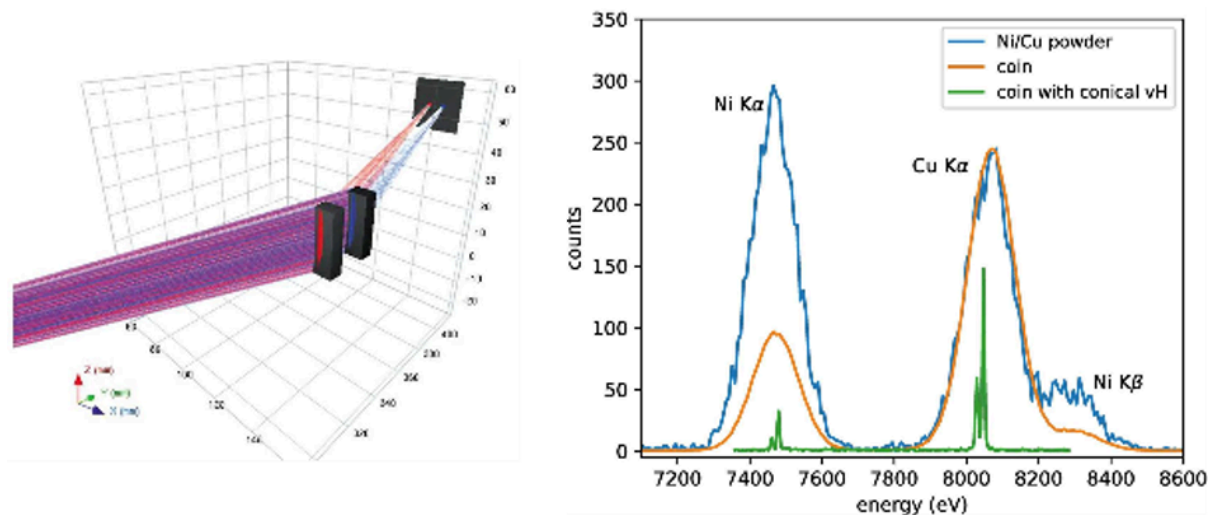


Figure Y. Ray-tracing simulation of the von Hámos spectrometer with the conical analyzer crystal set up to record Ni (red lines) and Cu (blue lines) emission spectra (left). Comparison of the XRF spectrum and the von Hámos high-energy-resolution XES spectrum (via the conical analyzer) of the inner part of a 200 HUF coin (right).

In addition to these two highlights, the members of the group published 14 further papers, mostly in Q1 journals.

## 2021

**Developments** — The group has been continuously developing theoretical and experimental tools in order to investigate the ultrafast photoinduced dynamics in functional molecules, and to design new ones with improved performance. The experimental tools include pioneering static high-energy-resolution laboratory X-ray spectroscopy, with hard X-ray absorption being performed routinely and efficiently, while X-ray emission spectroscopy is still being optimized. Ultrafast studies with X-ray spectroscopy and scattering probes are carried out at synchrotron radiation sources and X-ray free electron lasers, but we also participate in X-ray developments at the Extreme Light Infrastructure. In addition, we have realized in our home laboratory a femtosecond-resolved transient optical absorption spectroscopy station, and a femtosecond stimulated Raman scattering setup is being built. Our theoretical efforts focus on designing new functional molecules with quantum chemistry (which we later attempt to synthesize and then subject to experimental tests), as well as running (quantum) dynamics simulations to model the dynamics in light activated molecular systems. In what follows we report such works that were published in the previous year.

**Simulation of ultrafast excited-state dynamics in molecules.** — Time-resolved (TR) pump-probe experiments are very powerful tools to resolve ultrafast excited-state dynamics in functional molecules. However, the recorded TR data is very often complex and difficult to interpret, computations thus have a crucial role in extracting all important information from the measured data. Theory offers two fundamentally different approaches for the simulation of excited-state dynamics: i) quantum dynamics (QD), which is exact but only feasible for a few degrees of freedom, one is thus forced to develop reduced dimensionality models for molecules, and ii) semiclassical dynamics, which allows full dimensionality but in general, does not account properly for quantum effects. In an international collaboration, we employed trajectory surface hopping (TSH), which belongs to group ii), to simulate the photoinduced dynamics of trimethylamine (TMA) in full dimension, initiated from and occurring via Rydberg excited states [X1]. Importantly, the dynamics of TMA involve dissociation, for which the widely-utilized vibronic-coupling model of QD fails, but TSH does not. The utilized methodology is based on on-the-fly (time-dependent) density functional theory (DFT/TD-DFT) potential energy surfaces (PESs) and an energy-based technique to force an electronic transition near the  $S_1/S_0$  conical intersection (CI), in order to avoid single-reference failure of DFT at the CI. We concluded that electronic excitation into Rydberg states induces strong coherent vibrational umbrella motion, whose decoherence dynamics, in turn, controls the electronic relaxation and ballistic dynamics along the N-C bond. These N-C stretching dynamics can potentially open up for photodissociation, which is controlled by the branching at the  $S_1/S_0$  CI; we also found that the simulated dissociation yield depends heavily on the applied exchange-correlation functional. In a second work, we presented the first ab initio simulation of the entire singlet-triplet-quintet dynamics utilizing a synergistic TSH-QD methodology [X2]. For this study, we chose the octahedral  $[\text{Fe}(\text{NCH})_6]^{2+}$  complex, which is a model for Fe(II) low-spin (LS)  $\rightarrow$  high-spin (HS) photoswitching solely involving metal-centered excited states (Figure Xa). We here used full-dimensional TSH to select modes (see Figure Xb) for QD based on PESs and couplings calculated by high-level multiconfigurational quantum chemistry (CASPT2). The obtained mechanistic picture is consistent with experimental findings and includes assignment of the principal intermediate  $3T_2g$ , whose dynamics are controlled by the key Fe-N stretching vibrations.

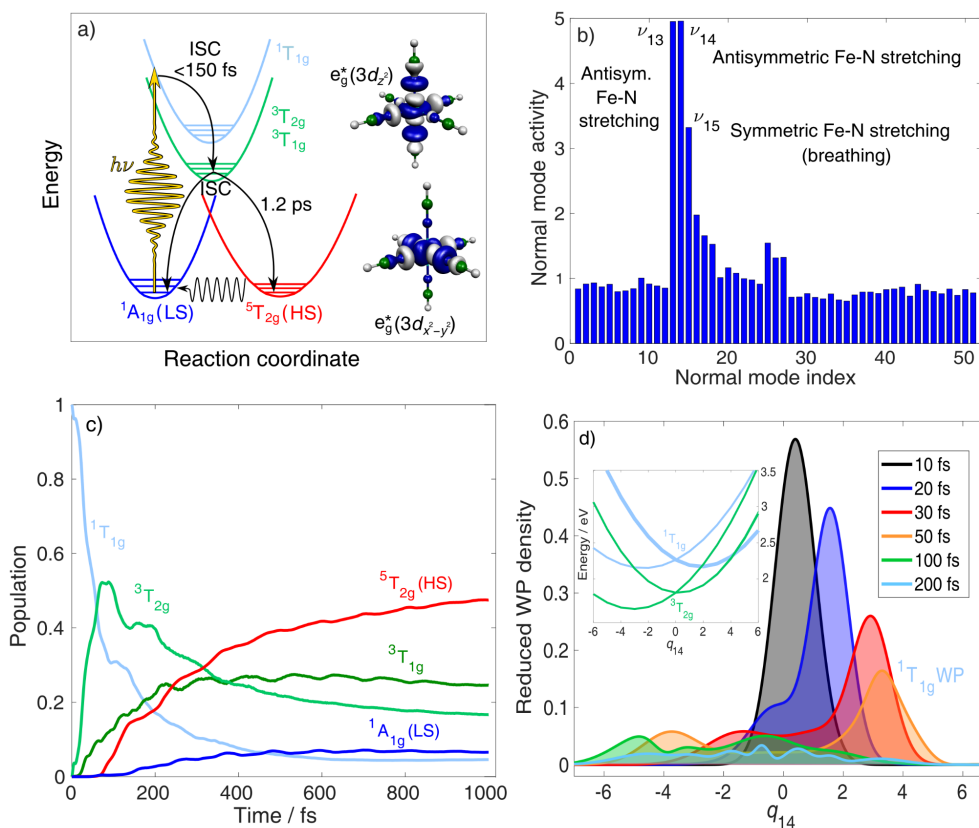


Figure X. Summary of the synergistic spin-vibronic simulations on the octahedral model  $[\text{Fe}(\text{NCH})_6]^{2+}$  for LS  $\rightarrow$  HS photoswitching. (a) Schematic mechanistic picture with the antibonding  $e_g^*$  orbitals illustrating the metal-center character of the excited states. (b) Mode selection by full-dimensional TSH (TD-DFT). (c) Population dynamics by 3D QD (CASPT2). (d) QD (CASPT2) along the antisymmetric Fe-N stretching normal mode coordinate  $q_{14}$ , illustrating singlet  $\rightarrow$  triplet ISC and wavepacket spreading. Adapted from ref. X2, the full article can be accessed at: <https://doi.org/10.1021/acs.inorgchem.1c01838>.

**Fs-resolved experiments and theoretical interpretation of nonadiabatic dynamics for small benchmark molecules.** — Calculation of time-dependent experimental observables, based on excited-state dynamics simulations, can be extensively used to interpret TR data. X-ray absorption spectroscopy (XAS) is an element and chemical state specific technique that is able to resolve electronic states and transitions between them. In an international collaboration, we assessed the performance of different electronic structure methods for the calculation of excited-state XAS of three benchmark molecules: uracil, thymine, and acetylacetone [X3]. We found that TD-DFT (B3LYP), utilizing the maximum overlap method (MOM) to obtain core-excited configurations that are inaccessible for TD-DFT referenced to the ground state, performs reasonably well. In combination with TSH, we used MOM-TD-DFT to simulate the TR-XAS of pyrazine, promoted to the  ${}^1\text{B}_{2u}(\pi\pi^*)$  to interpret a fs-resolved experiment. We found that in addition to  ${}^1\text{B}_{2u}(\pi\pi^*)$  and  ${}^1\text{B}_{3u}(n\pi^*)$  states, the debated optically-dark  ${}^1\text{A}_u(n\pi^*)$  state also participates in the electronic relaxation of pyrazine. We identified experimentally that the  ${}^1\text{A}_u$  state is populated in  $200\pm 50$  fs and is assigned by the 284.5 eV shoulder, red-shifted from the ground-state main peak by 0.9 eV, which, based on the XAS calculations, can only be attributed to  ${}^1\text{A}_u$  state (Figure Yc).

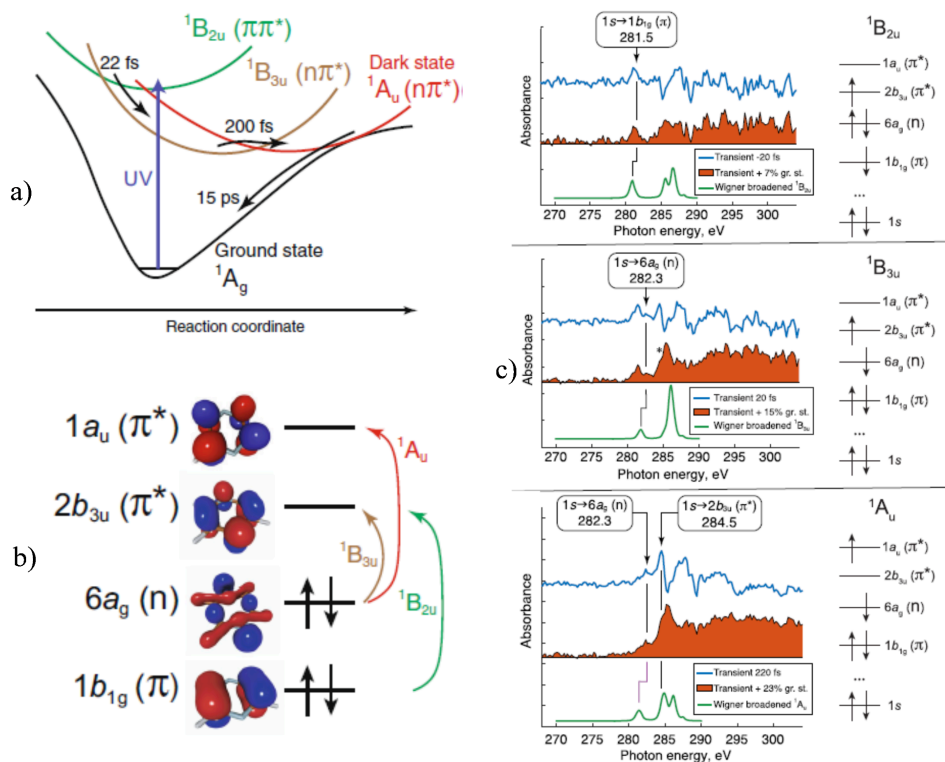


Figure Y. a) Schematic illustration of the excited-state dynamics of pyrazine with the experimental timescales; b) Dominant electronic character of the valence states  ${}^1B_{2u}$ ,  ${}^1B_{3u}$ , and  ${}^1A_u$ ; c) Experimental difference XAS (blue, pump-on – pump-off), the excited-state spectra, obtained by correction for ground-state bleach (orange filled area), and the simulated XAS for three selected time delays –20 fs, 20 fs, and 220 fs.

Also in an international cooperation we investigated the effect of non-adiabatic vibrational dynamics on resonantly enhanced multiphoton ionization. Time-resolved photoelectron spectroscopy (TR-PES) measurements on the benchmark CH<sub>2</sub>BrI molecule were interpreted in terms of 1D quantum dynamics simulation of the strong-field ionization dynamics, which include multiphoton resonance, dynamic Stark shifts, as well as vibrational dynamics and internal conversion during the ionization process. The theoretical model was based on the combination of the adiabatic elimination of off-resonant electronic states with the discretization of the ionic continua by Legendre polynomials of the photoelectron's kinetic energy. In agreement with the measured photoelectron spectra the simulations demonstrated how the ionization process can be controlled by phase-modulation of the exciting femtosecond near-infrared pulses. [Y1]

## References:

- [X1] Mátyás Pápai, Xusong Li, Martin M. Nielsen, Klaus B. Møller Trajectory surface-hopping photoinduced dynamics from Rydberg states of trimethylamine Phys. Chem. Chem. Phys., 23 (2021) 10964–10977.
- [X2] Mátyás Pápai Photoinduced Low-Spin High-Spin Mechanism of an Octahedral Fe(II) Complex Revealed by Synergistic Spin-Vibronic Dynamics Inorg. Chem. 60 (2021) 13950–13954.
- [X3] Shota Tsuru, Marta L. Vidal, Mátyás Pápai, Anna I. Krylov, Klaus B. Møller, Sonia Coriani An Assessment of Different Electronic Structure Approaches for Modeling Time-Resolved X-ray Absorption Spectroscopy Struct. Dyn. 8 (2021) 024101, (Special Issue „Theory of Ultrafast X-ray and Electron Phenomena”)
- [X4] Valeriu Scutelnic, Shota Tsuru, Mátyás Pápai, Zheyue Yang, Michael Ephstein, Tian Xue, Eric Haugen, Yuki Kobayashi, Anna I. Krylov, Klaus B. Møller, Sonia Coriani, Stephen R. Leone X-ray transient absorption reveals the  ${}^1A_u$  ( $n\pi^*$ ) state of pyrazine in electronic relaxation Nat. Commun. 12 (2021) 5003.
- [Y1] Brian Kaufman, Tamás Rozgonyi, Philipp Marquetand, Thomas Weinacht Competition between dynamic resonance and internal conversion in strong-field molecular ionization with chirped ultrafast laser pulses Phys. Rev. A 103 (2021) 023108.

---

2020

Light-activated functional molecules hold the promise for solutions to many technological problems ranging from IT to sustainable development. Relevant efforts have been focused on developing complexes of the abundant and environment-friendly iron, particularly on the ubiquitous model systems with polypyridine ligands. Finding suitable complexes for a targeted application is clearly a well-suited task for theory based ligand engineering, as in this approach a large number of compounds can be rapidly screened and evaluated at acceptable cost. The first steps for developing efficient light-activated functional molecules is to obtain a thorough understanding of their potential energy surfaces (PES), and unveil the relaxation pathways on them after the excitation. We report on some theoretical and experimental results on iron based molecules which shall assist to open new paths for developing molecular systems which are rather promising for applications.

In this report we first describe our work, which aimed to modify the excited quintet state lifetimes based on theoretical predictions; its experimental verification also constitutes our first published result from our home-built transient optical absorption spectroscopy setup. Secondly, we describe two insights into the light-excited dynamics of carbene complexes of iron, obtained with X-ray emission spectroscopy (XES) at an X-ray free electron laser (XFEL). Thirdly, we mention theoretical results which helped to rationalize ultrafast time-resolved measurements on benchmark halomethane molecules.

### Quantum-chemistry-aided ligand engineering for potential molecular switches [1]

For the applicability of Fe(II) based molecular systems of in future molecular switches the lifetime of the quintet state needs to be significantly increased from the values typically observed in Fe(II) complexes, and this in turn requires the modification of the potential energy landscape in such a way that the height of the energy barrier for the quintet to singlet relaxation is increased. This can be achieved in a systematic way by introducing electron withdrawing (EW) and donating (ED) substituents into the ligands of a given complex.  $[\text{Fe}(\text{terpy})_2]^{2+}$  (terpy = 2,2':6',2''-terpyridine) is a very promising parent complex, since its quintet state is already remarkably stable under special circumstances. For substitution we selected the 4' position, as changing the electron density on the central ring would likely have a large effect on the relaxation dynamics of the quintet state.

Having taken all the above factors into account, we set out to theoretically examine how the potential energy surfaces, and in consequence the lifetime of the excited quintet state of  $[\text{Fe}(\text{terpy})_2]^{2+}$  can be modified upon substitution with ED/EW groups in the 4' position. The theoretical predictions were verified by transient optical absorption spectroscopy.

Current quantum chemistry offers methods whereby very accurate potential energy surfaces can be calculated for both ground and excited states. However, those calculations are both expensive and require significant expertise, therefore they are not yet feasible for the purpose of ligand engineering, where we need to screen a large number of compounds and therefore need faster, simpler and cheaper methods. In this work we performed computationally undemanding DFT calculations to predict the energy minima of the ground and quintet excited states and to estimate the barrier height and the rate for the quintet to singlet relaxation of the substituted derivatives. As expected, we found that the various electron donating and withdrawing substituents have a significant effect on the energy difference between the singlet and quintet minima, thus substitution in the 4' position by these groups provides an opportunity to tune the energy gap. Subsequently we used the Arrhenius equation to determine from the barrier heights the relative lifetimes for the room temperature decay of the quintet states of the substituted derivatives compared to that of the parent compound.

In order to test the above concept experimentally, we have prepared the Fe(II) complexes with and determined the quintet lifetimes. For these experiments we employed our new, home built visible pump - supercontinuum probe femtosecond transient absorption setup, based on an amplified Ti:Sa laser system. The correspondence between the calculated quintet lifetimes and those determined from the transient absorption experiments is rather satisfactory, which demonstrates the validity of our approach towards estimating excited state lifetimes. One of the reasons for this good agreement is of course the great structural similarity between the set of complexes in our study.

Thus we have shown that by identifying the most relevant position for substitution and selecting suitable electron donating substituents it is possible to reshape the potential energy surfaces of the participating electronic states and thereby achieve an almost order of magnitude lengthening of the quintet lifetime in an Fe(II) terpyridine complex. One of the main results of this work is the successful demonstration that rational design of functional

molecules by quantum-chemistry-based ligand engineering is indeed possible using fast and affordable calculations.

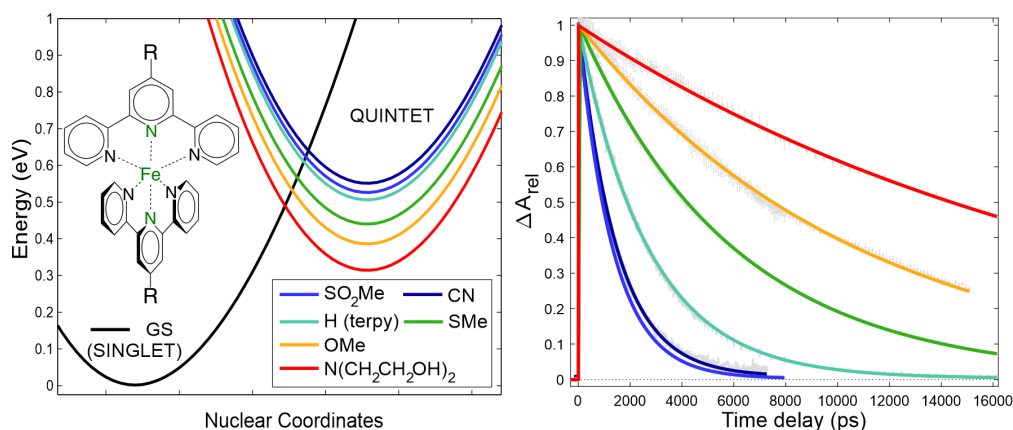


Figure 1. Singlet (ground state, 'GS') and quintet potential energy curves for  $[\text{Fe}(\text{terpy})_2]^{2+}$  derivatives substituted by different ED/EW groups at the 4' position, with R indicated in the legend, calculated at the DFT: B3LYP\*/TZVP level (left). Measured quintet decay curves of the complexes from transient optical absorption (right).

### XFEL results on ultrafast dynamics of photoexcited carbene complexes of iron

Based on our recent results on understanding and controlling the stability of transient states and decay pathways in optically excited functional iron-polypyridine-type complexes, the chemical environment of iron ions in such systems has been altered in order to significantly extend the lifetime of the intermediate excited states as desired for applications.

Firstly, a system designed to replace complexes of rare earths in light harvesting, the  $[\text{Fe}(\text{bimp})_2]^{2+}$  (bimp = 2,6-bis(3-methylimidazol-1-ylidene) pyridine) molecule was studied by femtosecond transient X-ray emission spectroscopy (XES, at the Fe K emission lines) and X-ray scattering in parallel. We detected oscillations of 278 fs period with both techniques in the first few picoseconds after the light excitation, which is the first case of observing ultrafast oscillations in XES. Theoretical calculations shed light on why the coherent nuclear dynamics of the metal-centered excited ( $^3\text{MC}$ ) state (populated after the first short lived (110 fs) metal to ligand charge transfer state (MLCT)), affects the XES. The experimental work was performed at the LCLS X-ray free electron laser.

The second work traces the branching pathways of a promising novel functional molecular system. Here we investigated the molecular ion  $[\text{Fe}(\text{bpy})(\text{btz})_2](\text{PF}_6)_2$  (bpy = 2,2'-bipyridine, btz = 4,4'-bis(1,2,3-triazol-5-ylidene)) also by ultrafast X-ray spectroscopy and X-ray scattering at the LCLS X-ray laser. In this case, we found that the  $^3\text{MLCT}$  state, which populates faster than ca. 100 fs, decays to the  $^3\text{MC}$  state partly directly and partly through another (cold)  $^3\text{MLCT}$  state, from where it returns to the ground state without reaching the usually dominant quintet excited state. The outstanding property of the system is that the lifetime of the ligand-excited state is significantly longer (7.6 ps) than that of the previous iron-polypyridine compounds, which is essential for solar energy utilization.

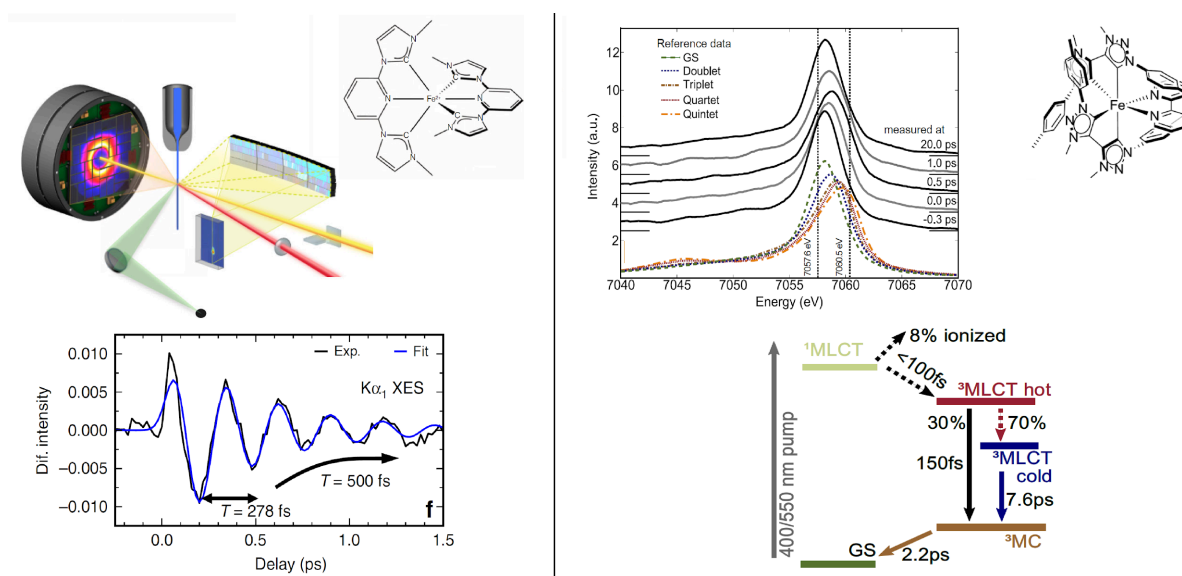


Figure 2. (left) Experimental setup for fs transient X-ray spectroscopy and scattering at LCLS and sketch of the  $[\text{Fe}(\text{bmip})_2]^{2+}$  molecular ion shown on top, extracted and fitted ultrafast oscillations on the Fe  $K\alpha_1$  XES line differences on the bottom (adapted from Ref. 2). (right) Top graph shows experimental Fe  $K\beta$  XES line of the depicted  $[\text{Fe}(\text{bpy})(\text{btz})_2]^{2+}$  molecule at different delays with reference spectra, bottom diagram demonstrates the suggested dynamics of the system after photoexcitation (adapted from Ref. 3).

## Theoretical study of light-induced nonadiabatic dynamics in complexes and dihalomethane molecules

Determining the possible photorelaxation pathways and estimating the lifetimes of the excited states is necessary for revealing the mechanism in functional molecules. A theoretical approach to this requires the simulation of the photorelaxation process, whereas for systems with a high density of excited states, such as several transition metal complexes, it might be necessary to explicitly account for the excitation process as well. Continuing our previous studies of iron complexes suggested as substitutes for the expensive and environmentally unfriendly rare earth-based photosensitizers for light-harvesting systems [4,5] we report taking this aspect into account in the ultrafast excited state relaxation dynamics of the  $[\text{Fe}(\text{bmip})_2]^{2+}$  (Figure 2) and the related  $[\text{Fe}(\text{btbip})_2]^{2+}$  complexes.

We also studied non-adiabatic dynamics in small benchmark molecular systems by high level quantum chemical computations in an international collaboration. With theoretical considerations based on these computations and dynamics simulations, several observations in various ultrafast time-resolved measurements on dihalomethane molecules (eg.  $\text{CH}_2\text{I}_2$ ,  $\text{CH}_2\text{BrI}$ ) were rationalized. Among others, the dynamics behind coherent control over internal conversion during resonantly enhanced strong-field multiphoton molecular ionization was explained and the maintenance of electronic coherence during the nonadiabatic transition was proved. (see Fig. 3) [6]

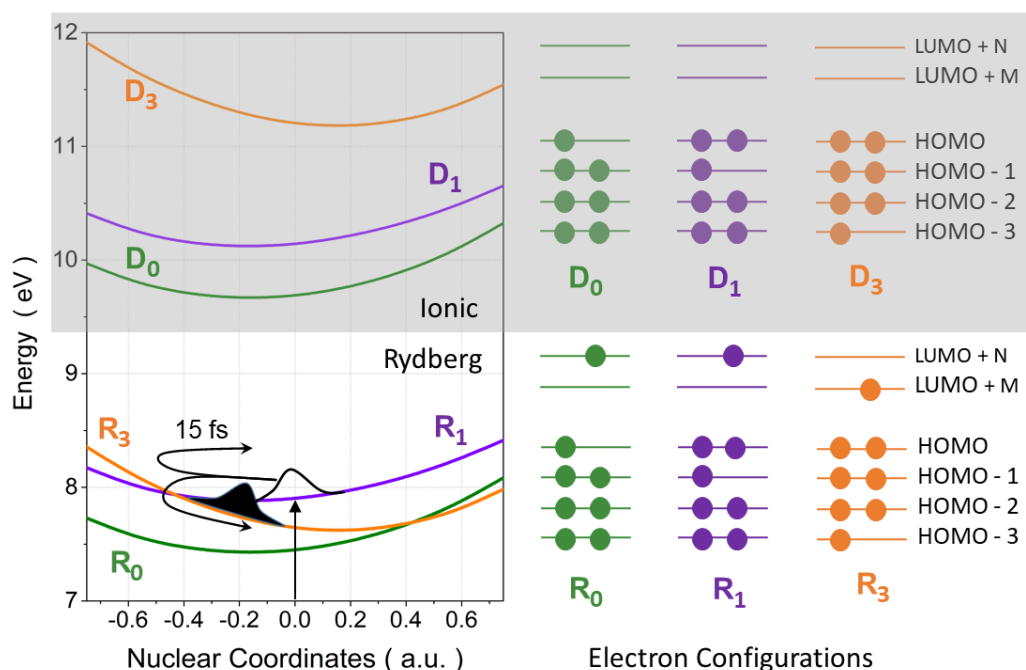


Figure 3. Potential energy curves along the wagging vibrational mode of  $\text{CH}_2\text{BrI}$  relevant to the wave packet dynamics during strong-field ionization are shown. Electron configurations of Rydberg ( $R_i$ ) and Dyson-correlated ionic ( $D_i$ ) states and the wave packet motion on the  $R_i$  potentials are indicated schematically. The wave packet excited by the pump pulse undergoes nonadiabatic transition from the upper to the lower Rydberg state and interferes with the wave packet excited by the probe pulse. This interference results in observable phase-dependent ionization to the different  $D_i$  states. [Adapted from Ref. 6]

## 2018

Developing light-activated functional molecules has been a major goal in molecular engineering, as such systems hold the promise for solutions to many technological problems ranging from IT to sustainable development. Relevant efforts have been focused on engineering complexes of the abundant and environment-friendly iron, particularly on the ubiquitous model systems with polypyridine ligands. The first steps for developing efficient light-activated functional molecules is to obtain a thorough understanding of their potential energy surfaces (PES), and unveil the relaxation pathways on them after the excitation. We report on some theoretical and

experimental results on iron based molecules which shall assist to open new paths for developing molecular systems which are rather promising for applications .

### Quantum nuclear wavepacket simulations of photoexcited Fe-carbene complexes

Determining the possible photorelaxation pathways and estimating the lifetimes of the excited states is necessary for revealing the mechanism in functional molecules. A theoretical approach to this requires the simulation of the photorelaxation process, whereas for systems with a high density of excited states, such as several transition metal complexes, it might be necessary to explicitly account for the excitation process as well. Continuing our previous studies of iron complexes suggested as substitutes for the expensive and environmentally unfriendly rare earth-based photosensitizers for light-harvesting systems [Pápai et.al. J. Phys. Chem. Lett. 7 (2016) 2009, J. Phys. Chem.C 120 (2016) 17234] we report taking this aspect into account in the ultrafast excited state relaxation dynamics of the  $[\text{Fe}(\text{btbip})_2]^{2+}$  and  $[\text{Fe}(\text{bmip})_2]^{2+}$  (Figure 1) complexes.

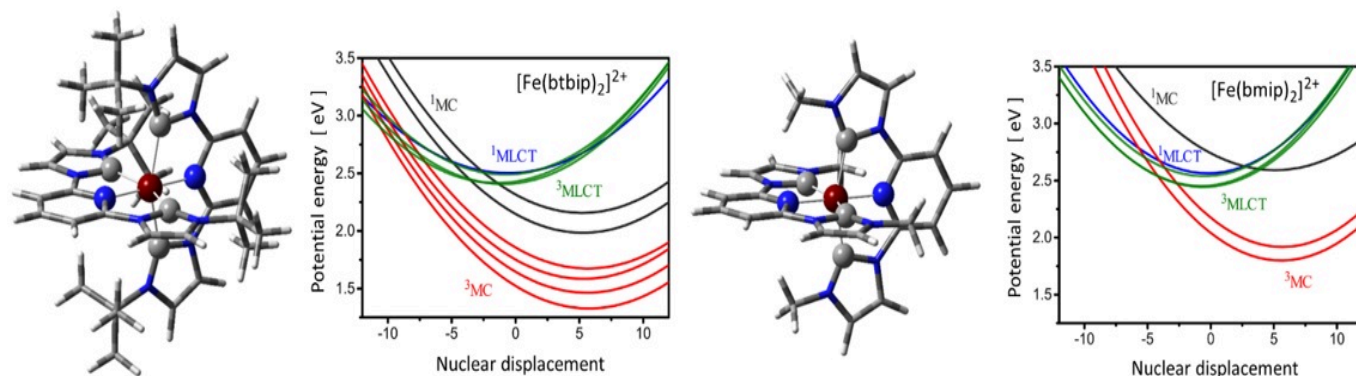


**Figure 1.** Molecular structures and potential energy curves for some excited states along the lowest frequency breathing vibrational mode of  $[\text{Fe}(\text{btbip})_2]^{2+}$  (btbip = 2,6-bis(3-tert-butyl-imidazole-1-ylidene)pyridine) (left) and  $[\text{Fe}(\text{bmip})_2]^{2+}$  (bmip = 2,6-bis(3-methyl-imidazole-1-ylidene) pyridine) (right). (N and C atoms are indicated by blue and grey colors, respectively.)

We performed quantum dynamics simulations in a four dimensional space spanned by the vibrational normal modes most relevant to the transitions. The current, improved description explicitly includes the interaction with the pump laser field in the Hamiltonian of the system in the semiclassical dipole approximation using transition dipole moments (TDM) obtained by the same time-dependent density functional theory (TD-DFT) method (B3LYP\*/TZVP) used also for computing the potential energy surfaces and the spin-orbit couplings (SOCs). The simulations were performed with the multi-configurational time-dependent Hartree (MCTDH) method in the vibrational coupling Hamiltonian (VCHAM) formalism. In this formalism the SOC and TDM vectors are directly determined by TD-DFT, while the non-adiabatic coupling terms and the parameters of the multidimensional potential energy surfaces are determined by fitting to TD-DFT adiabatic potential energy values. In both molecules, the optically bright singlet metal-to-ligand charge transfer state ( $^1\text{MLCT}$ ), as well as the energetically closest singlet metal-centred ( $^1\text{MC}$ ) states are degenerate, showing E symmetry. We have demonstrated that the spin-vibronic model, constructed directly from electronic structure calculations as described above, can exhibit erroneous, polarization-dependent relaxation dynamics for such degenerate states due to artificial interference of coupled relaxation pathways. We have shown that this problem stems from an incorrect description of the excitation of the ground state nuclear wavepacket into electronically degenerate states. The reason for this deficiency is that the simulation of the excitation process lacks rotational invariance implied by the symmetry of degenerate states. This translates into unphysical behavior through the nonadiabatic couplings among these states. We have demonstrated that a proper complex representation of TDMs is necessary to ensure rotational invariance of the excitation. This eliminates the unphysical interferences and thus produces correctly polarization-independent excited-state dynamics for both investigated complexes. Figure 2 shows the population dynamics for four simulations with different laser polarizations for which - without the correction - we obtained more than 20% deviations in excited state populations at 2 ps after the excitation and a difference of almost a factor of three in relaxation times.

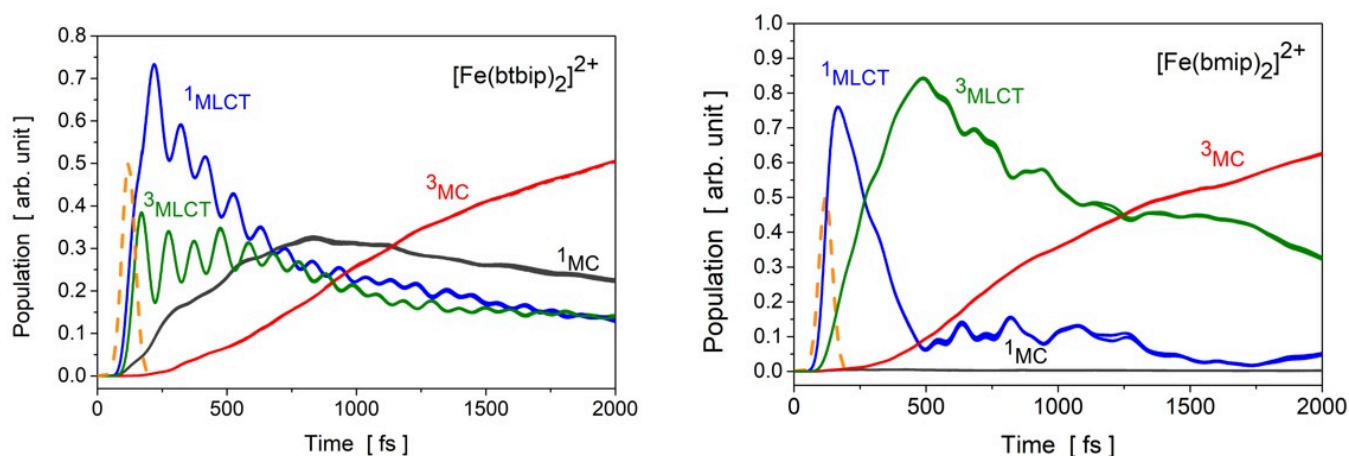


**Figure 2.** Results of the simulations: Excited state populations as a function of time for the  $[\text{Fe}(\text{btbp})_2]^{2+}$  (left) and  $[\text{Fe}(\text{bmip})_2]^{2+}$  (right) complexes following excitation by a 485 nm, 60 fs Gaussian pulse with four different laser polarizations. (The temporal intensity profile of the laser pulse is indicated by dashed orange line.) Due to the corrected description of the excitation process, no polarization dependence is observed. The paper can be downloaded from <http://dx.doi.org/10.1021/acs.jctc.8b00135>.

In agreement with related experiments [Liu et al. Chem. Comm. 49 (2013) 6412] the simulations reveal that an apparently minor structural difference considerably alters the relaxation dynamics in these functional complexes. In the present case, the tert-butyl group stabilizes the 1MC states, enabling the 1,3MLCT  $\rightarrow$  1MC population transfer in addition to the 3MLCT  $\rightarrow$  3MC pathway, which in turn leads to much faster relaxation of MLCT states. This explains the different photophysical behavior of these otherwise similar complexes, pointing out a crucial issue for tailoring the function in such complexes.

### Controlling the relaxation pathway in photoexcited transition metal complexes via substitution and solvent effects

An alternative way to alter the photophysical properties of transition metal complexes is to shift the potentials with solvent interactions. This can change the intersections of the potentials of and the couplings between different states, which will accordingly influence the transition trajectories and probabilities. Replacing two bipyridine ligands in the frequently studied  $[\text{Fe}(\text{bpy})_3]^{2+}$  (bpy = 2,2'-bipyridine) by 4 monodentate CN<sup>-</sup> ions introduces two effects that allows us to modify the PES. First, the CN<sup>-</sup> substitution makes the ligand field stronger, which shifts the MC (metal centered) states to higher energy; second, interaction with protic solvents affects the strength of the Fe–C bonds, which shifts the energy of the MLCT (metal-to-ligand charge transfer) states. We have investigated these effects on the  $[\text{Fe}(\text{bpy})(\text{CN})_4]^{2-}$  complex, in collaboration with the groups of Prof. Kelly Gaffney (SLAC) and Prof. M. Nielsen (DTU Lyngby), using a combination of transient optical absorption (TOAS) and X-ray emission spectroscopies. The first effect observed is that due to the increase in the ligand field, the MC states are destabilized, thus the potential energy landscape, as well as the relaxation pattern changes completely. While for  $[\text{Fe}(\text{bpy})_3]^{2+}$ , the relaxation follows a pattern the for the full photocycle 1GS  $\rightarrow$  1MLCT  $\rightarrow$  3MLCT  $\rightarrow$  3MC  $\rightarrow$  5MC  $\rightarrow$  1GS, with very short lived excited singlet and triplet states ( $\tau < 100$  fs), and a long lived (600 fs) quintet, the field enhancement of the 4 CN ligands shifts up the quintet to an unreachable energy, and makes the triplets longer lived. However, it depends on the solvent which triplet is stabilized. In water, a solvent with strong Lewis acidity/H-bonding ability, the MLCT excited state of  $[\text{Fe}(\text{bpy})(\text{CN})_4]^{2-}$  decays still rapidly, in less than 100 femtoseconds, forming a quasi-stable metal-centered excited state with 13 picosecond lifetime, while in weak Lewis acid solvents, such as dimethyl sulfoxide (DMSO) or acetonitrile, the same molecule possesses 19 picosecond 3MLCT excited state lifetime and no discernible contribution from MC states. It was shown that the MC excited state in the former case has triplet (3MC) character, unlike other reported six-coordinate Fe(II)-centered coordination compounds with a singlet ground state forming MC quintet (5MC) states. The influence of the solvent on the excited state relaxation dynamics arises from different solvent stabilization of the CN<sup>-</sup> ligand,

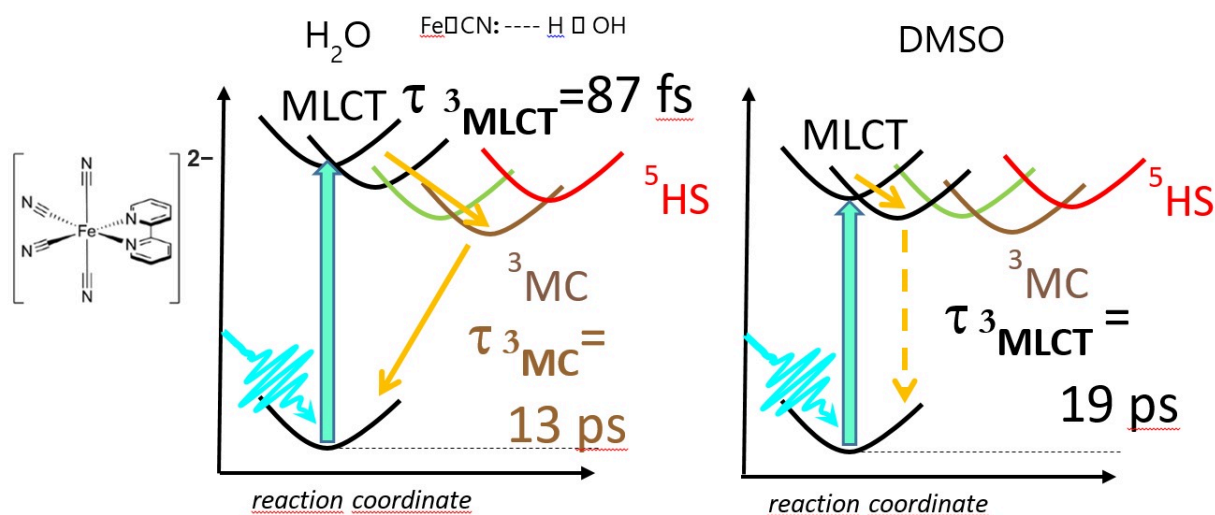


**Figure 3.** The  $[Fe(bpy)(CN)_4]^{2-}$  molecule (left), and its schematic potential energy curves for water (middle) and DMSO (right) solvents. Yellow arrows show the relaxation pathways. (The full article can be accessed at <http://dx.doi.org/10.1039/c7cp07838b>.)

which in turn modifies the relative energies of the MLCT potential energy curves, as shown in Figure 3. The observed solvent dependent changes in excited state non-radiative relaxation for  $[Fe(bpy)(CN)_4]^{2-}$  allows us to infer the influence of the solvent on the electronic structure of the complex.

Following the results detailed above, we have chosen to carry out a similar substitution on another model system,  $[Fe(terpy)_2]^{2+}$  (terpy: 2,2':6',2''-terpyridine) complex, whose photophysical behavior is well known [Pápai, M. et al., *J. Chem. Theory Comput.* 9, 509. (2013); Vankó, G. et al., *J. Phys. Chem. C*, 119 5888. (2015)]. The effect of the terpy – CN ligand substitution should in principle be the similar as described above for the bipyridine analogue, thus it should allow us to verify this type of controlling of the PES, hence the elementary processes of photorelaxation. Our theoretical (TD-)DFT and transient optical absorption studies on the  $[Fe(terpy)(CN)_3]^{-}$  system confirmed relevant variations in the PES and the time evolution, respectively, see the upper part of Fig. 4. Upon the cyanide substitution in  $[Fe(terpy)_2]^{2+}$ , the calculated triplet and quintet MC states are shifted to higher energies and the solvent effect on the MLCT bands is also reproduced (not shown here). TOAS reflect significantly different behavior compared to the original  $[Fe(terpy)_2]^{2+}$ , and also some difference from the bipy/CN mixed complex discussed above. Here the ligand field enhancement is somewhat smaller because of the smaller number of CN ligands, thus the quintet MC state is still reached in the relaxation, yet its small yield reflects small branching into this state. During one of the first pilot experiments at the European X-ray Free Electron Laser it was possible to perform a quick feasibility test on aqueous  $[Fe(terpy)(CN)_3]^{-}$  with 515 nm laser excitation and collect a delay scan of difference signals on the Fe K $\alpha$  lines. The lifetime obtained is fully consistent with that of the major component in the TOAS signal; however, better statistics, longer scan range and the collection of the K $\beta$  spectrum and wide angle scattering are required to fully characterize the excited state dynamics in these molecular systems.

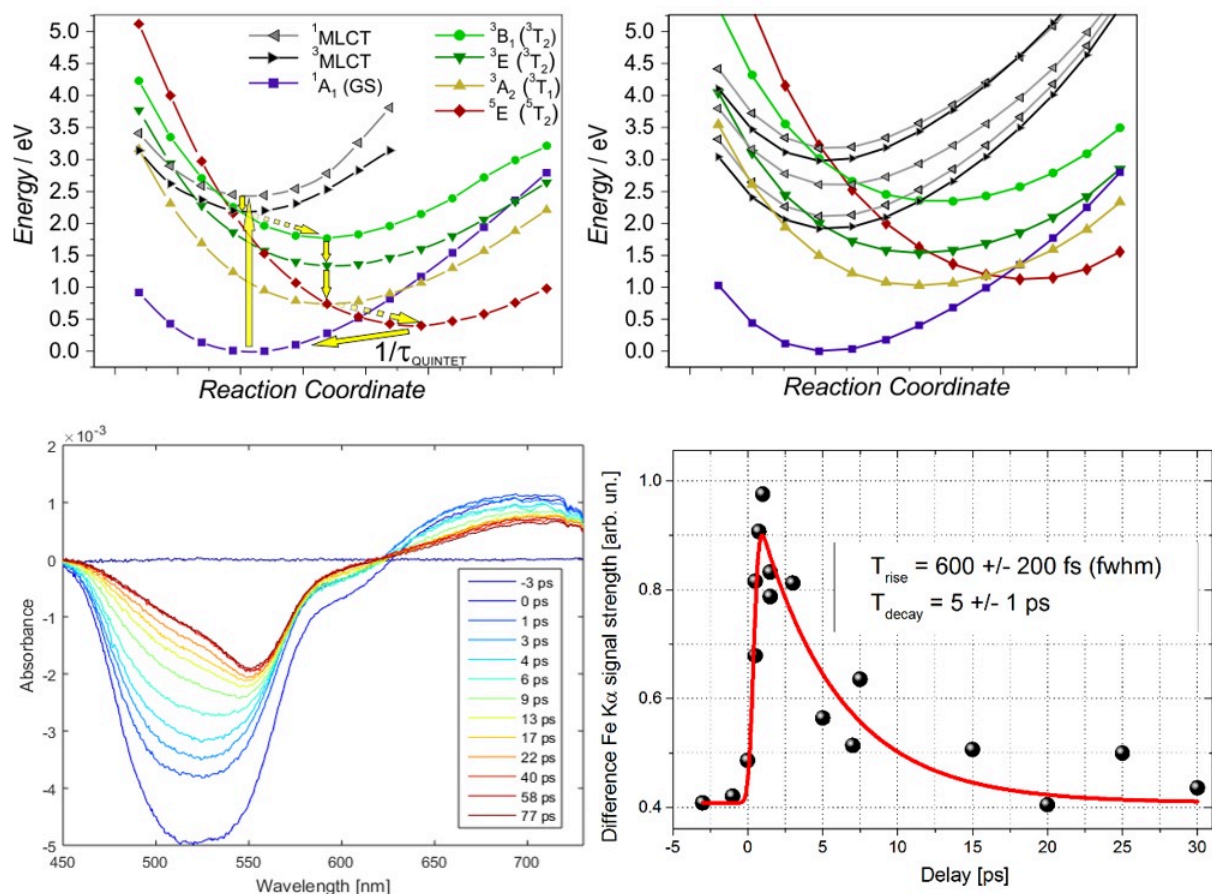


**Figure 4.** TOP: Calculated PES of the relevant ground-, MLCT, and MC excited states for  $[\text{Fe}(\text{terpy})_2]^{2+}$  (left) and for  $[\text{Fe}(\text{terpy})(\text{CN})_3]^-$  (right). BOTTOM: TOAS (left) and pilot XFEL data: K $\alpha$  XES difference signal of  $[\text{Fe}(\text{terpy})(\text{CN})_3]^-$  in water as a function of time delay (right).

## 2017

Hard X-ray spectroscopy is a powerful probe of the electronic and local atomic structure, combined with high penetration, element, orbital, and spin selectivity. Here we report on experimental results and technical developments using X-ray probes in investigations of transformations of transition metal complexes. First, we demonstrate valence-to-core X-ray emission spectroscopy as a novel ultrafast probe with high chemical sensitivity. Second, we show that laboratory spectrometers can do more than has been expected, monitoring the concentration dependence of the Ni speciation in solution with X-ray absorption spectroscopy. Finally, we show the realization of total reciprocity violation in the phase for photon scattering.

**Probing the dynamics of the valence electrons at a spin state in transition metal complexes.** — Pump-probe experiments are powerful structural dynamics tools, which apply an ultrashort laser excitation pulse, and study the time evolution of the system with a probe pulse at chosen time delays. Unveiling the details of the relaxation processes that follow the light excitation can lead to a complete understanding of the involved mechanisms, which, for instance, shall promote the design of more efficient functional molecules. Here we report on experimental results and technical developments using an X-ray probe in time-resolved investigation of a transition metal complex that is a model system for molecular switches; the experimental work is aided by quantum chemistry. We probed the dynamics of valence electrons in photoexcited  $[\text{Fe}(\text{terpy})_2]^{2+}$  complex in aqueous solution to gain deeper insight into the electronic structure changes that lead to changes of the Fe-ligand bonds using hard X-ray emission spectroscopy (XES). A picosecond-time-resolved measurement of the complete 1s X-ray emission spectrum captures the transient photoinduced changes and includes the weak valence-to-core (vtc) emission lines that correspond to transitions from occupied valence orbitals to the nascent core-hole. As DFT-calculations predict (Fig. 1A), vtc-XES offers particular insight into the molecular orbitals directly involved in the light-driven dynamics. As the result of the excitation, antibonding orbitals are populated and the metal ligand orbital overlap becomes weaker, resulting in intensity reduction as well as energy shift in the experiment (Fig. 1C), in excellent agreement with our calculations (Fig. 1B). More subtle features at the highest energies reflect changes in the frontier orbital populations. The results are shown in Figure 1.

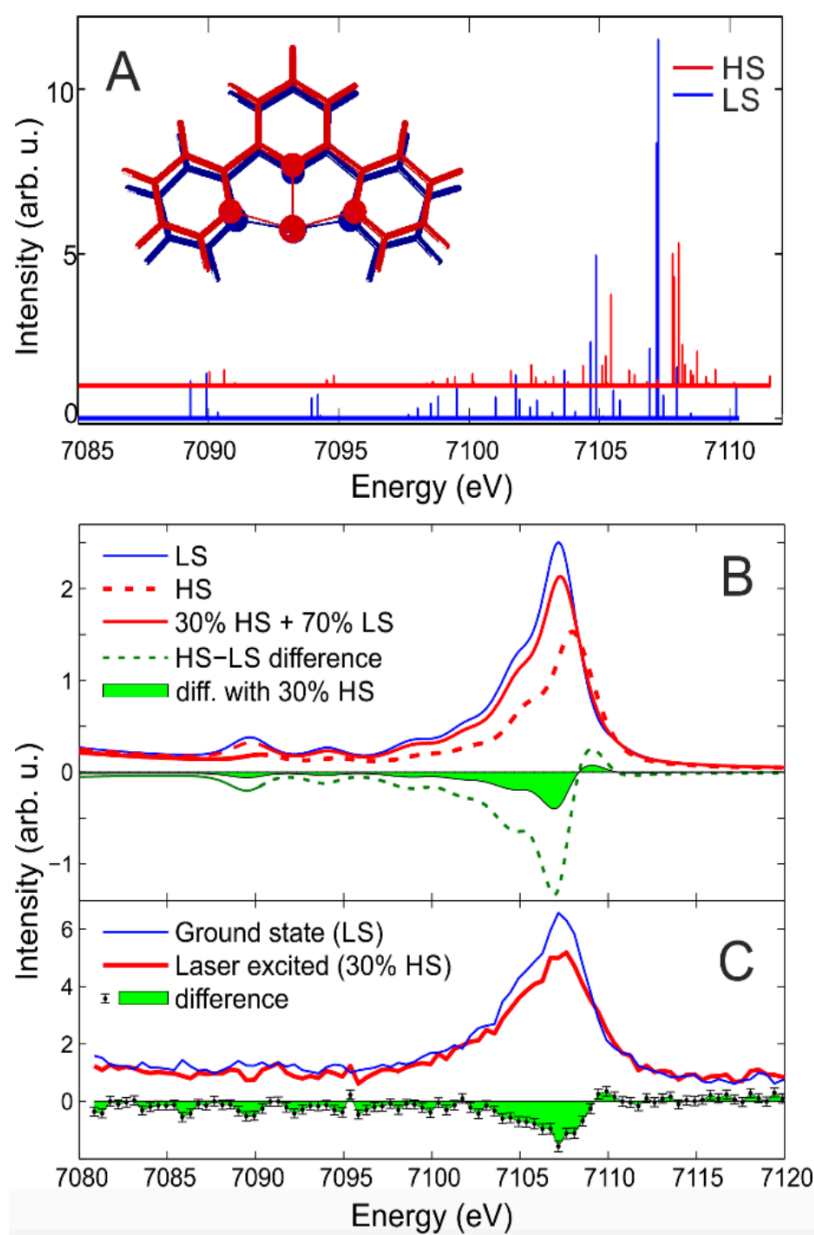
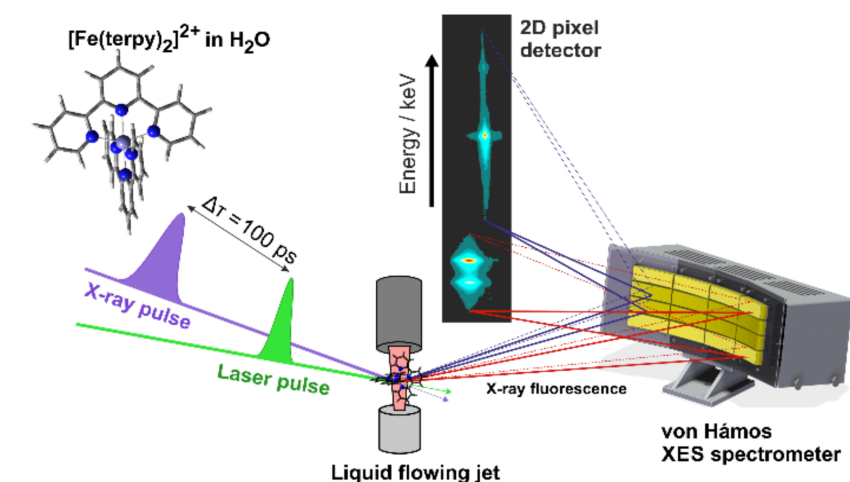


**Figure 1** (top) The experimental setup showing the 16-crystal von Hamos spectrometer installed in a pump-probe geometry. Two different sets of 8 Si analyzer crystals were used to collect both  $K\alpha$  and  $K\beta$  plus vtc X-ray emission simultaneously. The detector image shown is a cropped actual frame from the pixel detector recorded during the experiment. On the left the molecular structure of the  $[\text{Fe}(\text{terpy})_2]^{2+}$  complex is shown. **(A)** Stick diagram of the molecular orbital contributions to the vtc-XES spectra of LS and HS  $[\text{Fe}(\text{terpy})_2]^{2+}$  (blue and red,

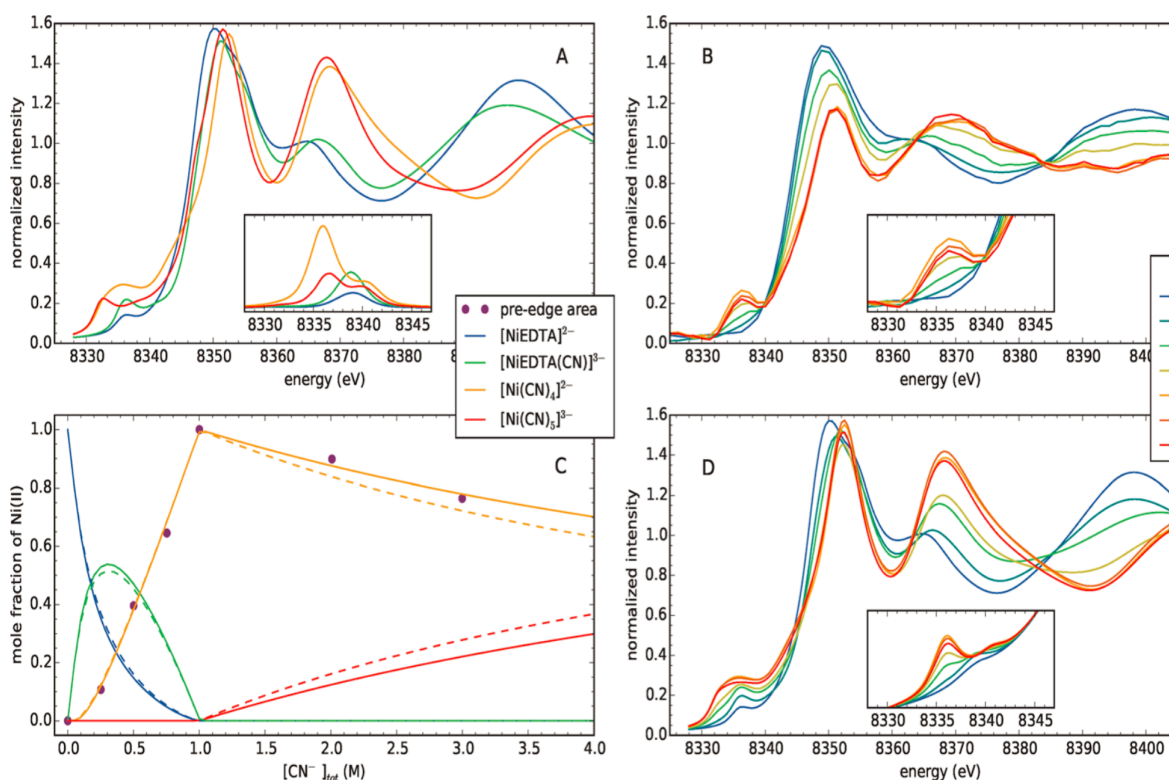
respectively). The variation of the molecular structure is also shown on an iron with a single terpy ligand. Calculated (B) and measured (C) vtc-XES spectra of LS and HS [Fe(terpy)<sub>2</sub>]<sup>2+</sup>.

This result demonstrates the potential of vtc-XES as an ultrafast probe, which, combined with femtosecond time resolution in future experiments at X-ray free electron lasers, will shed more light on the intricate details of the elementary transition processes. (The full article can be accessed at <http://dx.doi.org/10.1021/acs.jpcc.6b12940>.)

**Extending laboratory X-ray absorption spectroscopy for routine measurements in solution phase.** — A novel laboratory von Hámos X-ray absorption spectrometer had been built and tested with solid samples the previous year by the group. This year the spectrometer was applied to obtain structural data on liquid samples, thereby widening the range of laboratory measurements that previously could only have been performed at synchrotron sources. We successfully demonstrated on the Ni<sup>2+</sup> – EDTA – CN<sup>-</sup> ternary system that a complete speciation study can be performed from laboratory XANES (X-ray absorption near edge structure) measurement series, including the determination of the formation constants of the corresponding complexes. Moreover, the technique permits us to determine the local atomic structure around the Ni ion, with particular sensitivity to variations in symmetry. *To best of our knowledge this is the first time that laboratory X-ray absorption spectroscopy was used for such a comprehensive study in solution.*

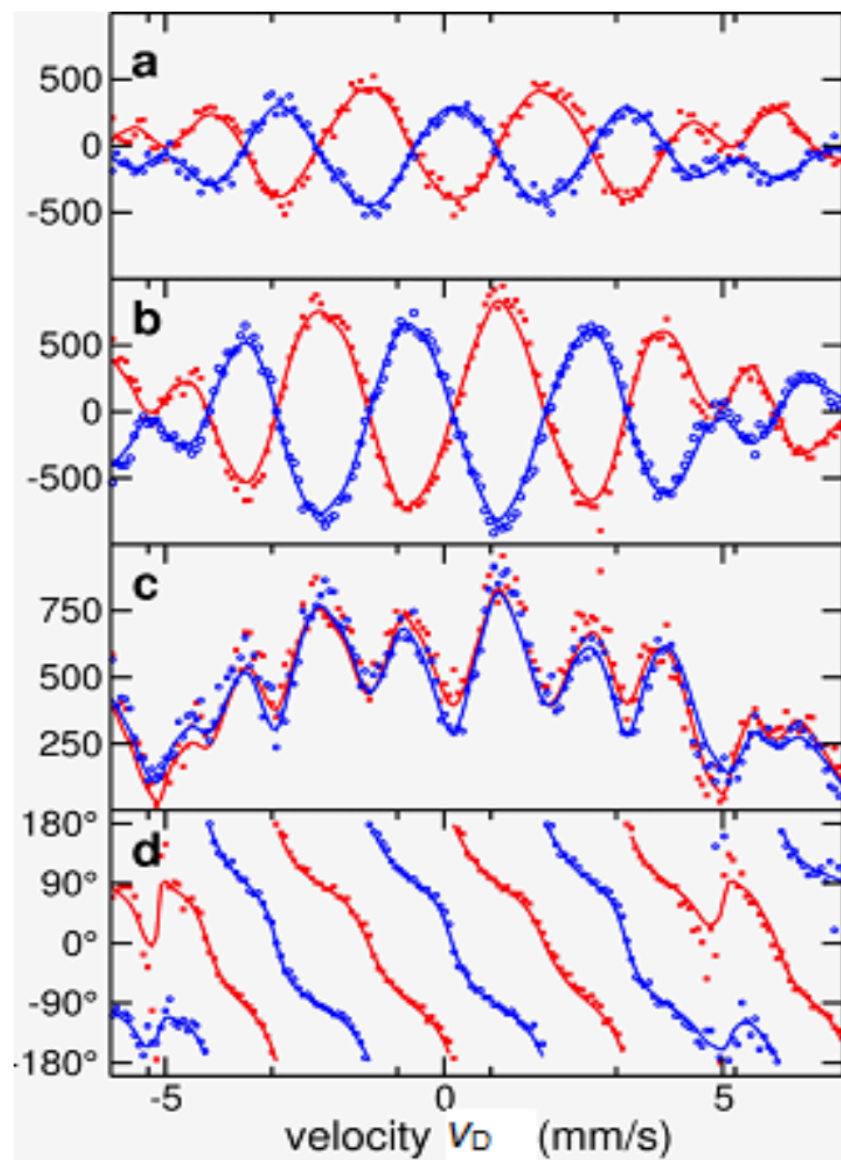
The NiII–EDTA–CN<sup>-</sup> (EDTA = ethylenediaminetetraacetic acid) ternary system, in spite of its fairly simple components and numerous investigations, can have several molecular combinations, all of them not being identified unambiguously beforehand. In order to achieve a detailed understanding of the reaction steps and chemical equilibria, methods are required in which the structural transitions in the different reaction steps can be followed via element-selective complex spectral feature sets. While standard optical spectroscopies failed to excel in this task, with the help of our recently developed von Hámos type high energy resolution laboratory X-ray absorption spectrometer, both the structural variations and stability constants of the forming complexes were determined from the same measurement series.

Figure 2 outlines the main results of the study. Fig. 2A shows the FEFF9 calculated XANES spectra for the [NiEDTA]<sup>2-</sup>, [NiEDTA(CN)]<sup>3-</sup>, [Ni(CN)<sub>4</sub>]<sup>2-</sup>, and [Ni(CN)<sub>5</sub>]<sup>3-</sup> complexes (the inset shows the preedge region for each complex calculated via TD-DFT/TDA), which were expected to appear in the studied concentration ranges of the different constituents. Panel B shows the experimentally recorded spectra for a series of NiII–EDTA–CN<sup>-</sup> mixtures with different CN<sup>-</sup> concentrations. In the inset a significant change of the preedge features with a peak around 8336 eV can be observed, representing the formation of four- and/or five-coordinated nickel(II) complexes. From the relative areas of these preedge peaks, the ratio of the tetra- as well as the pentacyanide Ni complexes could be deduced, which is compared to literature based calculated distributions. Based on this distribution, the calculated XANES spectra for the measured samples could be reconstructed (panel D), which agree remarkably well with the experimental ones in panel B.



**Figure 2.** (A) Calculated XANES spectra of the four base complexes. (B) Laboratory XANES spectra of solutions containing constant 0.25 M NiCl<sub>2</sub> and 0.30 M EDTA, while the concentration of the added KCN was varied between 0 and 3 M. (C) Distribution diagram of the following species: [NiEDTA]<sup>2-</sup> (blue), [NiEDTA(CN)]<sup>3-</sup> (green), [Ni(CN)<sub>4</sub>]<sup>2-</sup> (yellow), and [Ni(CN)<sub>5</sub>]<sup>3-</sup> (red). The dashed lines stand for the calculated-, the continuous ones for the XANES preedge fitted distributions. (D) Calculated XANES spectral series for the measured samples based on the determined nickel distribution shown in (C). (The full article can be accessed at <http://dx.doi.org/10.1021/acs.inorgchem.7b02311>.)

**Realizing total reciprocity violation in the phase for photon scattering.** — The reciprocity principle requires the scattering amplitude to be symmetric for the transposition of the detector and the source. While reciprocity involves the interchange of source and detector, it is fundamentally different from rotational invariance, and is a generalization of time reversal invariance, occurring in absorptive media as well. Reciprocity can be proved as a theorem in many situations and is found violated in other cases. For polarization dependent scatterings reciprocity is often violated, but violation in the phase of the scattering amplitude of X-ray photons oscillating in the attosecond range is much harder to experimentally observe than violation in magnitude.



**Figure 3.** Real part (a), imaginary part (b), magnitude (c) and phase (d) of the complex scattering amplitude. The figure displays the range of the -1st order stroboscopic resonances; dots are experimental signals and continuous lines are theoretical simulations. The agreement between direct (red) and reciprocal (blue) data visible in (c) demonstrates magnitude reciprocity, while (d) shows maximal reciprocity violation in the phase (red and blue curves running with a 180° phase difference).

Enabled by the advantageous properties of nuclear resonance scattering of synchrotron radiation (SR), a maximal - i.e., 180-degree - reciprocity violation in the phase was found. For accessing phase information a new version of stroboscopic detection of nuclear resonance scattering of SR was developed. The scattering setting was devised based on a generalized reciprocity theorem that opens the way to construct new types of reciprocity

related devices. The experiment realizing the direct and reciprocal scattering processes was performed at the High Resolution Dynamics Beamline P01 of the PETRA-III synchrotron source of the Deutsches Elektronen Synchrotron (DESY). The beam was scattered on a pair of  $^{57}\text{Fe}$  containing foils placed between a polarizer and an analyser, both having an extinction of  $10^{-8}$ , and was subsequently detected by a Si avalanche photo diode. One of foils was a single-line stainless steel absorber mounted on a Mössbauer drive, and the other foil produced the polarization dependent scattering as a result of being magnetic. Each of the six high-frequency and narrow nuclear resonance signals in the magnetic foil gets superposed and produces beats with the corresponding nearby frequency resonance signal in the reference foil. These lower frequency beats are not only more easily detectable but, thanks to the heterodyne setup, also tuneable by the Doppler shift of energy caused by the  $v_D$  velocity of the Mössbauer drive. After a pulse, resonances decay as time passes, and one detects counts – essentially, intensity – as a function of time as well as of the drive velocity. This intensity gets multiplied, in the stroboscopic evaluation, by appropriate window functions and then integrated giving spectra shown in Fig. 3. The predicted  $180^\circ$  phase difference between direct and reciprocal data is apparent in Fig. 3d. (*The full article can be accessed at <http://dx.doi.org/10.1038/srep43114>.*)